Resonance-enhanced multiphoton ionization photoelectron spectroscopy of Rydberg states of N_2O below the $X^2\Pi$ ionization limit

Scheper, C.R.; Kuijt, J.; Buma, W.J.; de Lange, C.A.

DOI
10.1063/1.477431

Publication date
1998

Document Version
Final published version

Published in
Journal of Chemical Physics

Resonance-enhanced multiphoton ionization photoelectron spectroscopy of Rydberg states of N_2O below the $X\ ^2\Pi$ ionization limit

C. R. Scheper, J. Kuijt, W. J. Buma, and C. A. de Lange
Laboratory for Physical Chemistry, University of Amsterdam, Nieuwe Achtergracht 127-129, 1018 WS Amsterdam, The Netherlands

(Received 16 March 1998; accepted 5 August 1998)

A three-photon resonance-enhanced multiphoton ionization spectroscopic study on N_2O is carried out in the spectral range from 80 000 cm^{-1} up to the lowest ionization limit at 103 963 cm^{-1}. High-resolution photoelectron spectroscopy is used to identify and characterize the observed excited states. Eighteen origins are reported which have either not been assigned before or are reassigned now. Moreover, the photoelectron spectra taken at higher-lying resonances often show extensive vibronic coupling with the near-resonant vibronic manifolds built on lower-lying origins. © *1998 American Institute of Physics.* [S0021-9606(98)01042-3]

I. INTRODUCTION

As an all first-row-element triatomic molecule with $C_{\infty v}$ symmetry in both the neutral and ionic ground states, N_2O is very much suited for detailed quantum-mechanical and spectroscopic investigation. The present study of the N_2O molecule complements a series of recent resonance-enhanced multiphoton ionization photoelectron spectroscopy (REMPI-PES) studies on other 16-valence electron systems with a linear structure: CO_2, COS, and CS_2.[1–3] Investigation of N_2O is also of interest from an environmental point of view, as the molecule plays an important role in atmospheric processes.[4,5]

The configuration of the electronic ground state ($X\ ^1\Sigma^+$) of N_2O is given by

$$\ldots 6\sigma^2 1\pi^4 7\sigma^2 2\pi^4.$$

The lowest adiabatic ionization energy (IE) has been determined by a number of methods, including extrapolation of Rydberg series,[6] photoelectron spectroscopy,[7] mass detection of N_2O^+ (appearance potential),[8,9] and pulsed field ionization (PFI) in combination with electron detection.[10] The most accurate value is $103\,963 \pm 5$ cm^{-1}, which is given by the latter method. Due to spin-orbit coupling, the ionic ground state is split into two terms, $X\ ^2\Pi_{3/2}$ and $X\ ^2\Pi_{1/2}$, the latter of which lies 134 cm^{-1} higher than the former.[10] The vibrational frequencies of the N_2O and N_2O^+ ground states are given in Table I. If the doubly degenerate bending vibration ν_2^+ is excited, the electronically two-fold degenerate $X\ ^2\Pi_{3/2}$ and $X\ ^2\Pi_{1/2}$ spin-orbit components of the ground state ion are split, due to the interaction of the electronic orbital angular momentum Λ and the vibrational angular momentum ℓ, which is the so-called Renner–Teller effect.[11] Analysis of emission spectra ($X\ ^2\Pi \leftarrow A\ ^2\Sigma^+$) of N_2O^+ has led to precise energy values for the $\nu_2^+ = 1$ vibronic levels.[12] The adiabatic IE for formation of the first excited ionic state $A\ ^2\Sigma^+$ is given as 16.38(9) eV (132 185 cm^{-1}) by photoelectron spectroscopy.[7]

Quite a number of techniques, including photoabsorption,[6,13,14] electron impact[15,16] and resonance-enhanced multiphoton ionization in combination with mass-resolved ion detection (REMPI)[17,18] have been used for spectroscopic investigation of the excited states of N_2O below the $X\ ^2\Pi$ limit. Studies on superexcited states include photoionization[9] and measurement of fluorescence from excited neutral fragments as a function of the excitation wavelength.[19]

The first comprehensive study of the N_2O absorption spectrum was performed by Duncan,[13] in the spectral region of 45 455–117 647 cm^{-1}. He found three regions of continuous absorption and a number of discrete bands. The maxima of two continua at 77 900 and 91 200 cm^{-1}, respectively, together with the bands at 95 852, 98 326, 99 609, and 100 379 cm^{-1}, were taken as members of a Rydberg series converging to the first ionization limit and fitted to the following formula:

$$E/hc = 102567 - R/(n-0.92)^2, \quad n = 3,4,\ldots,8.$$

However, Duncan used an erroneous value of 102 567 cm^{-1} (12.72 eV) for the series limit, as was first noted by Watanabe,[8] who reported a value of 12.90 eV, close to its present value. Whether the observed resonances form a series is therefore questionable. Duncan's observations were largely confirmed by those of Lassettre *et al.*[15] and Zelikoff *et al.*[14] The latter group studied the wavelength region between 47 619–92 593 cm^{-1} in more detail and reported a number of additional bands.

Extensive Rydberg structure was reported by Tanaka *et al.*[6] in the energy range between 84 600–161 300 cm^{-1}. They arranged the observed bands in nine series, converging to the $X\ ^2\Pi$, $A\ ^2\Sigma^+$, and $C\ ^2\Sigma^+$ ion cores. A number of bands found by the above-mentioned authors[6,13–15] have been assigned by Lindholm[20] in $nl\lambda$ terminology on the basis of expected quantum defects for particular types of Rydberg orbitals. Moreover, Berkowitz and Eland[9] observed several Rydberg series converging to the $A\ ^2\Sigma^+$ and $C\ ^2\Sigma^+$ limits in their photoionization spectra, which were not reported by Tanaka *et al.*[6]

TABLE I. Fundamental frequencies (cm^{-1}) of the symmetric stretch (ν_1), the bending (ν_2), and the asymmetric stretch (ν_3) vibration, in the ground state of neutral N_2O and N_2O^+.

		N_2O ($X\ ^1\Sigma^+$)	N_2O^+ ($X\ ^2\Pi_{3/2}$)	N_2O^+ ($X\ ^2\Pi_{1/2}$)
ν_1		1284.91[a]	1126.51[a]	1126.42[a]
ν_2		588.77[a]		
	$^2\Sigma^+$		412.354[b]	
	$^2\Delta_{5/2}$		449.477[b]	
	$^2\Delta_{3/2}$		579.269[b]	
	$^2\Sigma^-$		619.259[b]	
ν_3		2223.76[a]	1737.6[a]	1737.7[a]

[a]Reference 27.
[b]Reference 12.

More recently, Patsilinakou *et al.*[17] used resonance-enhanced multiphoton ionization in combination with mass-resolved ion detection (REMPI) to investigate the range from 80 000 to 90 000 cm^{-1}. Their spectra suggested new origins ($3p\sigma\ ^1\Pi$; $3p\pi\ ^1\Sigma^+$, $^1\Delta$; $3d\sigma\ ^1\Pi$; $3d\pi\ ^1\Sigma^+$, $^1\Delta$ and $3d\delta\ ^1\Pi$, $^1\Phi$) and a wealth of vibronic structure mainly associated with the $3p\sigma\ ^1\Pi$ origin.

Szarka and Wallace,[18] who investigated the range from 80 000 to 87 000 cm^{-1} using the same technique, largely confirmed or refined the tentative assignments of Patsilinakou *et al.* and assigned some new vibronic structure associated with the $3p\sigma\ ^1\Pi$ state. Their analysis includes labeling of the resonances with vibronic term symbols, and was assisted by comparing intensities and band contours using linearly and circularly polarized light.

In the present work, Rydberg states in the energy range from 80 000 cm^{-1} up to the lowest IE at 103 963 cm^{-1} are detected by (3+1) REMPI in combination with mass-resolved ion detection or kinetic-energy-resolved photoelectron detection. The application of high-resolution photoelectron spectroscopy to these Rydberg states has enabled us to identify the final ionic states reached in the photoionization process, so that an unambiguous assignment of the observed resonances can be made. Moreover, near-resonant vibronic interactions between (high-lying) Rydberg states and the vibronic manifolds built on lower-lying origins can be observed in the photoelectron spectra.

For the majority of the bands observed between 80 000 and 90 000 cm^{-1}, we confirm the assignments of Patsilinakou *et al.*[17] and Szarka and Wallace.[18] However, some bands are reassigned. The range from 90 000 cm^{-1} up to the lowest ionization limit is investigated with the REMPI-PES technique for the first time. In this spectral region we find a large number of origins, including 17 origins which were either not assigned earlier or are reassigned now. Most of the observed states belong to Rydberg series converging to the lowest IE ($X\ ^2\Pi$), but one resonance is assigned as a state built upon the $A\ ^2\Sigma^+$ ionic core.

II. EXPERIMENT

The experimental setup has been described in detail previously.[21] Briefly, the laser system consists of a Lumonics HyperDye 500 dye laser (bandwidth ~0.08 cm^{-1}) operating on DMQ, PTP, DCM, Rhodamine B, or Rhodamine 6G, which is pumped by a XeCl excimer laser (Lumonics HyperEx 460) operating at 30 Hz. The dye laser output is frequency-doubled, when necessary, in a Lumonics HyperTrak 1000 unit using a KD*P or BBO crystal. The output radiation is focused ($f.l.=25$ mm) into a ''magnetic bottle'' photoelectron spectrometer, which alternatively can be used as a time-of-flight mass spectrometer. In the case of electron detection, the magnetic bottle spectrometer allows for a collection efficiency of 50%. The laser wavelength, as well as the energy scale of the photoelectrons, was calibrated using resonance-enhanced multiphoton ionization of krypton or xenon via known excited states.[22] An energy resolution of typically 10–18 meV (FWHM) was achieved for krypton and xenon. N_2O (Matheson) was effusively introduced into the spectrometer.

III. RESULTS AND DISCUSSION

A. Rydberg structure between 80 100–86 400 cm^{-1}

The three-photon excitation spectrum in the range between 80 100–86 400 cm^{-1} is obtained using kinetic-energy-resolved photoelectron detection. The observed band positions are in good agreement with the data of Patsilinakou *et al.*[17] and Szarka and Wallace.[18] The observed bands were assigned by these authors as the $3p\sigma\ ^1\Pi$ origin and vibronic structure belonging to it. By analysis of the photoelectron spectra recorded at the maxima of all the resonances, we are able to confirm their assignments for the majority of the observed bands. However, our spectra show that the previous assignments of the bands at 82 725 and 83 882 cm^{-1} as 3_1^1 and $2_0^1\ ^1\Delta$ transitions, respectively,[17,18] are not correct.

The photoelectron spectrum taken at the resonance of 82 725 cm^{-1} shows a doublet (split by 131 cm^{-1}) with energies of 0.769 and 0.786 eV [see Fig. 1(a)]. These energies are compatible only with transitions to $X\ ^2\Pi_{1/2}$ (0,0,0) and $X\ ^2\Pi_{3/2}$ (0,0,0), respectively, starting from the vibronic ground level of N_2O. Therefore, this resonance is identified as an origin, but with a signal intensity which is low compared to that corresponding to the $3p\sigma\ ^1\Pi$ origin at 83 178 cm^{-1}. We therefore identify the intermediate state at 82 725 cm^{-1} as the $3p\sigma\ ^3\Pi$ origin. This assignment differs from the previous one, where this feature was assigned as a 3_1^1 band associated with the $3p\sigma\ ^1\Pi$ origin.[17,18]

The photoelectron spectrum at 83 882 cm^{-1} [see Fig. 1(b)] shows peaks with kinetic energies of 0.868 and 0.884 eV (prominent feature) and of 0.952 and 0.968 eV (weak doublet). The kinetic energies of the weak doublet are consistent with formation of $X\ ^2\Pi_{3/2}$ (0,0,0) and $X\ ^2\Pi_{1/2}$ (0,0,0) starting from $X\ ^1\Sigma^+$ (0,0,0). The largest peak in the photoelectron spectrum is split by 129 cm^{-1}, suggesting formation of $X\ ^2\Pi_{3/2}$ and $X\ ^2\Pi_{1/2}$, both with an internal energy of 678 cm^{-1}. The position of the resonance in the excitation spectrum, 704 cm^{-1} above the $3p\sigma\ ^1\Pi$ origin, together with the observations in the photoelectron spectrum, suggest that the feature is built on the $3p\sigma\ ^1\Pi$ origin. However, a definitive assignment cannot be made, since there is no likely vibronic level available to explain the observed ion internal energies. A $3_1^1 1_0^1$ hot band transition fits the energy requirements, but

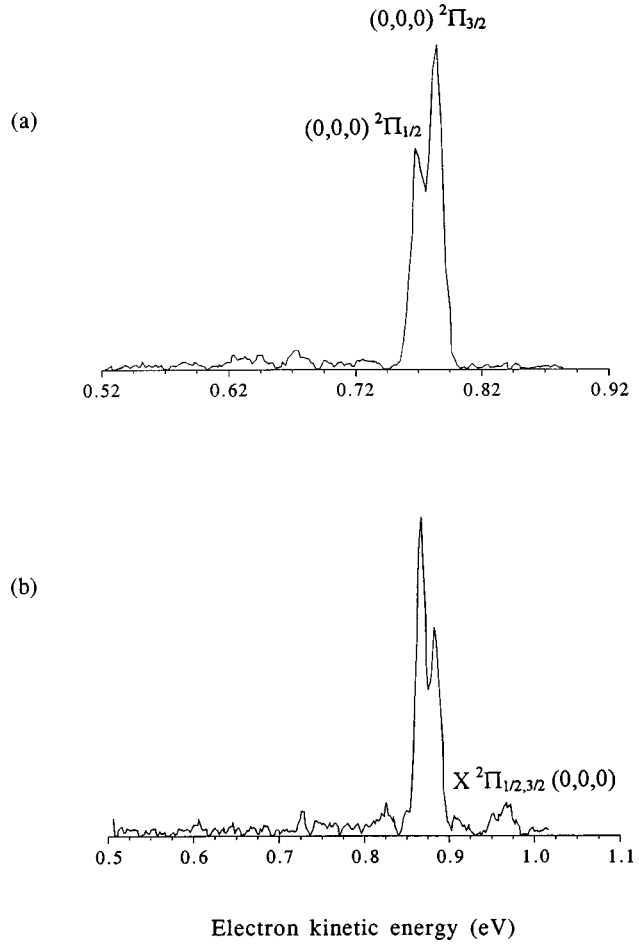

FIG. 1. Photoelectron spectra resulting from (3+1) REMPI via the resonances at a) 82 725 cm^{-1} and b) 83 882 cm^{-1}.

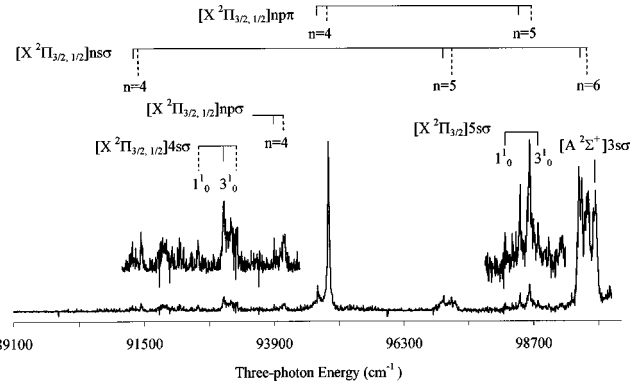

FIG. 2. (3+1) REMPI spectrum from 89 100 up to 100 050 cm^{-1}, obtained by monitoring the N_2O^+ mass channel. Proposed assignments of the origins and associated vibronic structure are given in the uncoupled [ion core]$n\ell\lambda$ representation. Dashed lines indicate $\Omega_c = 1/2$ cores.

seems unlikely because the $X\ ^1\Sigma^+$ (0,0,1) level of N_2O is not expected to be populated significantly at room temperature. In any case, on the basis of the photoelectron spectrum the previous assignment of this feature at 83 882 cm^{-1} to a $2^1_0\ ^1\Delta$ band[18] cannot be correct. Also, as noted by Szarka and Wallace,[18] the splitting of 272 cm^{-1} between the $2^1_0\ ^1\Sigma^+$ and $^1\Delta$ terms in the REMPI spectrum is larger than expected for a level split by Renner–Teller interaction.

B. Rydberg structure between 89 100–100 050 cm^{-1}

Figure 2 shows the three-photon excitation spectrum in the range of 89 100–100 050 cm^{-1} obtained by monitoring the N_2O^+ ion channel. Selecting the electrons of interest appeared to be difficult in this wavelength region, due to a larger yield of electrons arising from ionization of various fragments. Therefore, mass-resolved ion detection is applied, although our spectrometer allows for a higher collection efficiency in the case of electron detection.

The resonances observed in the excitation spectrum are assigned as $ns\sigma(n=4-6)$, $4p\sigma$, and $np\pi(n=4,5)$ Rydberg states built upon the $[X\ ^2\Pi_{1/2}]$ or the $[X\ ^2\Pi_{3/2}]$ ionic core. Some of these origins have been found previously: the $[X\ ^2\Pi_{1/2}]np\pi$ $(n=4,5)$ and $[X\ ^2\Pi_{3/2}]np\pi$ $(n=4,5)$ states have been reported by Tanaka *et al.*,[6] while the $[X\ ^2\Pi_{1/2}]ns\sigma$ $(n=4,5)$ states have been observed by Lassettre *et al.*[15] The excitation spectrum also shows vibronic structure associated with these Rydberg states. An interloper resonance is observed at 99 830 cm^{-1}, previously reported by Tanaka *et al.*[6] at 99 710 cm^{-1}, which has been identified as the $[A\ ^2\Sigma^+]3s\sigma$ state by Lindholm.[20] Intensities are determined to a large extent by the dye that is used, and by the position of the resonances on the dye gain curve. Since we made no special effort to compensate for these effects, nothing can be inferred with certainty concerning the relative intensities of the resonances. Some wavelength regions could not be covered well by any dye, which has inhibited as yet the observation of some Rydberg states (e.g., $5p\sigma$, $6p\sigma$, and $6p\pi$). In this work no clear evidence for $[X\ ^2\Pi_{3/2,1/2}]nd$ series with members expected in the same energy region was found.

Photoelectron spectra were used again to allow the identification of the resonant states. No difficulties were encountered in assigning most of the resonances, but a small number of them proved to be difficult, as will be discussed below. Despite the fact that sometimes quite weak features in the excitation spectrum are addressed, the corresponding photoelectron spectra and the observed quantum defects are mostly quite informative. Only in a few cases, e.g., the weak features at ~91 865 cm^{-1}, the PE spectra remained inconclusive.

The photoelectron spectrum recorded at 91 283 cm^{-1} shows three weak peaks with almost equal intensity. The peaks at 2.199 and 2.055 eV can be attributed to formation of $^2\Pi_{3/2}$ (0,0,0) and $^2\Pi_{3/2}$ (1,0,0), respectively, starting from $X\ ^1\Sigma^+$ (0,0,0). The peak at 2.285 eV is not easy to explain. The peak could be attributed to an overlapping hot band transition, but there is no obvious transition fulfilling the energy requirements. Another possibility is that the peak is due to ionization of a fragment. The fact that the resonance is an origin is confirmed by the photoelectron spectrum recorded at 91 443 cm^{-1}, which unambiguously identifies this resonance as an origin with an $\Omega_c = 1/2$ core. This band is assigned as the $[X\ ^2\Pi_{1/2}]4s\sigma$ state. From its position, the resonance at 91 283 cm^{-1} must therefore be its $\Omega_c = 3/2$, ''triplet'' counterpart. The assignment of the resonances at 91 283 and 91 443 cm^{-1} is further supported by the features

at 92 486, 92 971, and 93 181 cm^{-1}. The positions in the REMPI spectrum and the kinetic energies in the photoelectron spectra of these resonances identify them as, respectively, an 1_0^1 transition associated with the $[X\ ^2\Pi_{1/2}]4s\sigma$ state and 3_0^1 transitions associated with both the $\Omega_c=3/2$ and $\Omega_c=1/2$ states.

The photoelectron spectrum recorded at 94 075 cm^{-1} shows weak peaks at 2.643 and 2.656 eV, compatible with a 0_0^0 transition to the $X\ ^2\Pi_{1/2}$ and $X\ ^2\Pi_{3/2}$ states, respectively. The most intense feature at 2.399 eV, however, seems to indicate formation of $X\ ^2\Pi_{3/2}$ with an internal energy of 2165 cm^{-1}, or formation of $X\ ^2\Pi_{1/2}$ with an internal energy of 2033 cm^{-1}. Again, no obvious vibronic transition fulfills the energy requirements. The peak might be due to near-resonant vibronic coupling with a lower-lying origin at approximately 92 000 cm^{-1} (*vide infra*), but there is no clearly resolved resonance at this position in the REMPI spectrum. The band at 94 075 cm^{-1} is identified as the $[X\ ^2\Pi_{1/2}]4p\sigma$ state, but the assignment is not reliable since the origin of the most prominent feature in the photoelectron spectrum is unclear.

In Fig. 2, three resonances are observed at 99 561, 99 692, and 99 830 cm^{-1}. The photoelectron spectra recorded at 99 561 and 99 692 cm^{-1} clearly show that these resonances belong to series converging to the lowest IE. However, electrons with comparable kinetic energies are absent for the resonance at 99 830 cm^{-1}. We therefore conclude that this resonance does not belong to a series converging to the lowest IE. Convergence to the $A\ ^2\Sigma^+$ limit would mean production of electrons with very low kinetic energy (0.115 eV). Indeed, a weak signal corresponding to electrons with low kinetic energy (approximately 0.34 eV) is present in the photoelectron spectrum. Lindholm[20] lists a band at 99 770 cm^{-1} and assigns it as a $3s\sigma$ origin built upon the $A\ ^2\Sigma^+$ ionic core. Since it proved to be difficult to determine such a low kinetic energy with adequate precision under the present experimental conditions, we are inclined to support the previous assignment of the resonance as a transition to the vibrationless $[A\ ^2\Sigma^+]3s\sigma$ state.

Surprisingly, the photoelectron spectrum of the resonance at 99 830 cm^{-1} shows a strong signal when the filter, used to separate the frequency-doubled from the fundamental laser radiation, is removed. Under these conditions, both the doubled and undoubled output are available for spectroscopy. From this we conclude that undoubled light is used in the ionization step of this feature. Using this undoubled radiation, we find transitions in the photoelectron spectrum at kinetic energies of 1.546 and 1.530 eV, indicating formation of $X\ ^2\Pi_{3/2}$ (0,0,0) and $X\ ^2\Pi_{1/2}$ (0,0,0). We explain these observations as a $3+1'$ resonance-enhanced transition to an autoionizing state in the Franck–Condon gap between the $X\ ^2\Pi$ and $A\ ^2\Sigma^+$ limits.

C. Rydberg structure between 100 800–104 200 cm^{-1}

The three-photon excitation spectrum in the 100 800–104 200 cm^{-1} energy region, obtained by monitoring the N_2O^+ ion channel, is depicted in Fig. 3. The photoelectron spectra, recorded at the maxima, identify all resonances as origins.

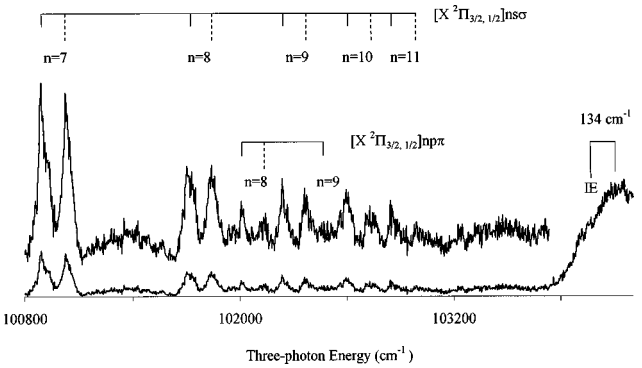

FIG. 3. (3+1) REMPI spectrum from 100 800 up to 104 200 cm^{-1}, obtained by monitoring the N_2O^+ mass channel. Proposed assignments are given in the uncoupled [ion core]$n\ell\lambda$ representation. Dashed lines indicate $\Omega_c=1/2$ ion cores.

The observed resonances in this wavelength region are assigned as $ns\sigma(n=7-11)$ and $np\pi(n=8,9)$ Rydberg states converging to the $X\ ^2\Pi_{3/2}$ or the $X\ ^2\Pi_{1/2}$ limit. The $[X\ ^2\Pi_{3/2}]np\pi(n=8,9)$ states have been reported previously by Tanaka *et al.*[6]

An overview of the positions of the maxima ($\overline{\nu}$) of the origins in the 3+1 REMPI spectra is presented in Table II together with their effective principal quantum number ($n^*=n-\delta$, where n is the principal quantum number and δ the quantum defect), which is calculated using the relationship $\overline{\nu}=\text{IE-R}/(n^*)^2$, where R is the Rydberg constant (109 737 cm^{-1}). The ionization limit IE in this expression is taken as 103 963 or 104 097 cm^{-1},[10] depending on whether the com-

TABLE II. Effective principal quantum numbers n^* and proposed assignments for the origins in the (3+1) REMPI spectrum. Newly assigned origins are printed in bold type. The series are denoted in an (uncoupled) [ion core]$n\ell\lambda$ representation and, in parentheses, in a (coupled) Hund's case *a* or *b* representation. The lowest-lying states are best described by the coupled representation. When going to higher excitation energies, the [ion core]$n\ell\lambda$ representation becomes the most appropriate.

Transition energy (cm^{-1})	n^*	n	Transition energy (cm^{-1})	n^*	n
$[X\ ^2\Pi_{3/2}]ns\sigma\ (^3\Pi)$			$[X\ ^2\Pi_{1/2}]ns\sigma\ (^1\Pi)$		
91 283	2.94	$n=4$	91443	2.94	$n=4$
97 034	3.98	$n=5$	97207	3.99	$n=5$
99 561	4.99	$n=6$	**99 692**	4.99	$n=6$
100 889	5.99	$n=7$	**101 039**	5.99	$n=7$
101 727	7.01	$n=8$	**101 846**	6.98	$n=8$
102 252	8.01	$n=9$	**102 378**	7.99	$n=9$
102 604	8.99	$n=10$	**102 754**	9.04	$n=10$
102 872	10.03	$n=11$	**103 008**	10.04	$n=11$
$[X\ ^2\Pi_{3/2}]np\sigma\ (^3\Pi)$			$[X\ ^2\Pi_{1/2}]np\sigma\ (^1\Pi)$		
82 725	2.27	$n=3$	83 178	2.29	$n=3$
93 904	3.30	$n=4$	**94 075**	3.31	$n=4$
$[X\ ^2\Pi_{3/2}]np\pi\ (^3\Sigma^+)$			$[X\ ^2\Pi_{1/2}]np\pi\ (^1\Sigma^+)$		
94 705	3.44	$n=4$	94 903	3.45	$n=4$
98 449	4.46	$n=5$	98 623	4.48	$n=5$
102 019	7.51	$n=8$	**102 136**	7.48	$n=8$
102 474	8.58	$n=9$			
$[A\ ^2\Sigma^+]ns\sigma\ (^1\Sigma^+)$					
99 830	1.84	$n=3$			

panion photoelectron spectrum identifies the Rydberg state as being associated with a series converging to the $X\ ^2\Pi_{3/2}$ or $X\ ^2\Pi_{1/2}$ spin-orbit state of the ion.

The calculated quantum defects of the $[X\ ^2\Pi_{3/2}]ns\sigma\ ^3\Pi$ and $[X\ ^2\Pi_{1/2}]ns\sigma\ ^1\Pi$ series are in the range of 0.97–1.06 and 0.96–1.06, respectively. The theoretically obtained value for the $ns\sigma$ series in N_2O is 1.04.[23]

The series designated as $[X\ ^2\Pi_{3/2}]np\sigma\ ^3\Pi$ and $[X\ ^2\Pi_{1/2}]np\sigma\ ^1\Pi$ have quantum defects of 0.7, clearly identifying the Rydberg orbitals as $np\sigma$ or $np\pi$. Polarization studies[18] suggest a Π term for the $n=3$ singlet origin, thereby identifying the Rydberg orbital as $np\sigma$.

D. Additional considerations

Going from low to high principal quantum numbers transition from Hund's case *a* or *b* to Hund's case *c* is expected to take place.[24] In low *n* Rydberg states, exchange interactions make a significant contribution to the observed splitting between the $\Omega_c=$'1/2' and $\Omega_c=$'3/2' states. As a result, the singlet–triplet character is largely preserved. Therefore, the singlet state will be dominant in the REMPI spectrum.

In high *n* Rydberg states, the exchange energy is nearly zero. In this case, the mixing between the singlet and the triplet levels is nearly complete, and the splitting between them is approximately equal to the ground-state ionic spin-orbit splitting. As both states have mixed singlet–triplet character, they have equal intensity in the REMPI spectrum. Another indication of a transition to Hund's case *c* can be obtained from the photoelectron spectra. The photoelectron spectrum will show only one core if Hund's case *c* is appropriate.

Although the splitting in the excitation spectrum between the $[X\ ^2\Pi_{3/2}]ns\sigma$ and $[X\ ^2\Pi_{1/2}]ns\sigma$ states is quite irregular, probably due to the weakness of some signals and overlapping series, it has a mean value close to 134 cm^{-1} for $n=6$ and higher. For $n=4$ and $n=5$, the splitting seems to be significantly larger than the spin-orbit splitting in the ground-state ion. This would imply that there is still some contribution from the exchange interaction to the observed splitting, and thus that transition to Hund's case *c* is not yet complete. Since the $\Omega_c=3/2$ and the $\Omega_c=1/2$ states are nearly equal in strength in the REMPI spectrum, even for $n=4$ and $n=5$, we conclude that Hund's case *c* labeling is appropriate for all observed origins of these series (though to a somewhat lesser extent for $n=4$ and $n=5$), which is also indicated by the photoelectron spectra. Turning to the $np\sigma$ series, the REMPI and photoelectron spectra show that the $3p\sigma\ ^1\Pi$ and $3p\sigma\ ^3\Pi$ states are best described in Hund's case *a* or *b* terms. The observed splitting in the excitation spectrum for the $n=4$ origins of these series is 171 cm^{-1}, indicating that Hund's case *c* labeling starts to become appropriate in the $np\sigma$ series for $n=4$ and higher.

The series designated as $[X\ ^2\Pi_{3/2}]np\pi\ ^3\Sigma^+$ and $[X\ ^2\Pi_{1/2}]np\pi\ ^1\Sigma^+$ show splittings of 198, 174, and 117 cm^{-1} for $n=4$, $n=5$, and $n=8$, respectively, suggesting that the transition to Hund's case *c* (Ref. 24) is completed somewhere between $n=5$ and $n=8$. Also, the intensities of the features, both in the excitation spectra and in the associated photoelectron spectra, support this point of view. They

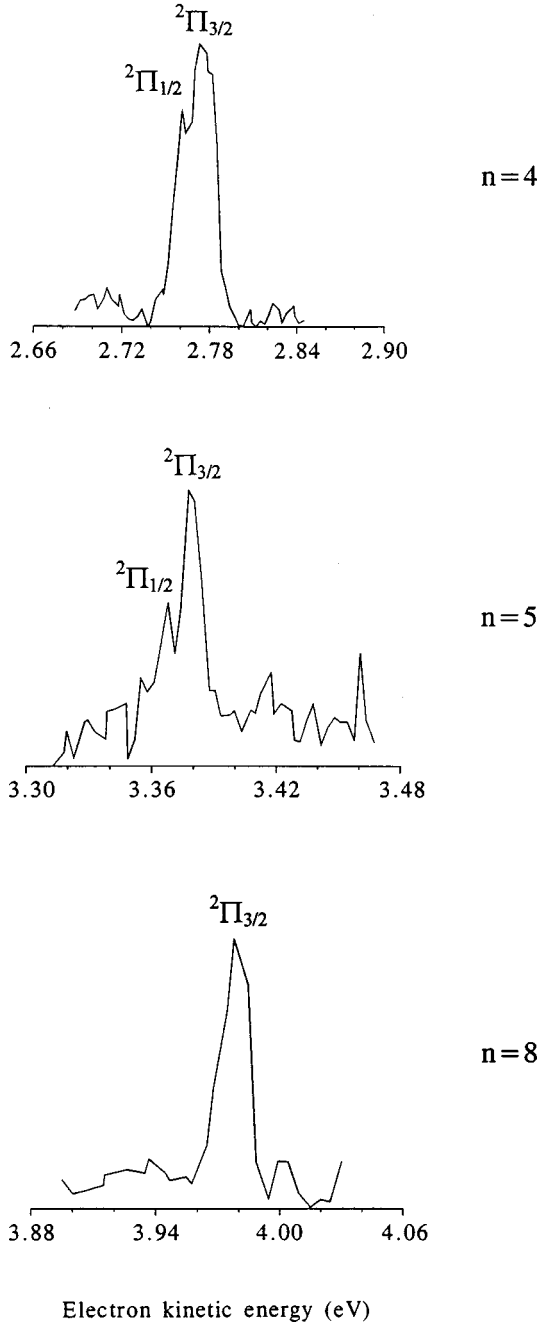

FIG. 4. Photoelectron spectra resulting from (3+1) REMPI via the $n=4$, $n=5$, and $n=8$ members of the $[X\ ^2\Pi_{3/2}]np\pi$ series.

clearly show that for $n=4$ the singlet–triplet mixing is still weak with the singlet dominating, while for the higher $n=5$ and $n=8$ members of the $[X\ ^2\Pi_{3/2,1/2}]np\pi$ series, increased singlet–triplet mixing develops. The photoelectron spectra of the $n=4$, 5, and 8 members of the $[X\ ^2\Pi_{3/2}]np\pi$ series are depicted in Fig. 4, which shows the transition to Hund's case *c*. In Hund's case *a* or *b* representation, $^{1,3}\Delta$ and $^{1,3}\Sigma^+$ terms are possible for these series. As the resonances are also present in the one-photon absorption spectrum,[6] we label them in Table II as $^3\Sigma^+$ and $^1\Sigma^+$.

The $np\pi$ series were first observed by Tanaka *et al.*,[6] who labeled them as series I and II. Their series show quite

irregular splittings. Starting with a splitting of 327 cm^{-1} for $n=3$, the splitting decreases to 156 cm^{-1} for $n=5$ (as expected for a transition to Hund's case *c*), but then goes up again, reaching splittings of 230 and 290 cm^{-1} for $n=8$ and $n=9$, respectively. We suggest that some assignments of Tanaka's higher-lying origins are not correct.

In one particular case, this is clearly shown by the photoelectron spectra. In the REMPI spectrum (Fig. 3), a resonance can be observed with its maximum at 102 019 cm^{-1}, in good agreement with the resonance assigned as $n=8$, series I by Tanaka *et al.* at 101 990 cm^{-1}. The photoelectron spectrum shows formation of $X\ ^2\Pi_{3/2}$ (0,0,0) only. The $n=8$, series II resonance is reported at 102 220 cm^{-1}, nearly coinciding with the resonance we assigned as $[X\ ^2\Pi_{3/2}]9s\sigma$ at 102 252 cm^{-1}. That this resonance cannot belong to series II ($\Omega_c=1/2$ core) follows from the photoelectron spectrum, which exclusively shows the $X\ ^2\Pi_{3/2}$ (0,0,0) core. In addition, a resonance 117 cm^{-1} above the one at 102 019 cm^{-1} is observed, which predominantly shows formation of $X\ ^2\Pi_{1/2}$ (0,0,0). We assign *this* resonance as $[X\ ^2\Pi_{1/2}]8p\pi$.

It is interesting to note that N_2O is in many ways similar to CS_2. Both molecules have a 16-electron valence shell, and the highest occupied molecular orbital (HOMO) cannot be approximated by an atomic orbital. Since CS_2 belongs to the $D_{\infty h}$ point group, there are marked differences between its 2+1 and 3+1 REMPI spectra due to the parity selection rules: only the $np\sigma_u$, $np\pi_u$, and $nf\lambda_u$ series are observed in the 3+1 REMPI spectrum, whereas the 2+1 REMPI spectrum shows only the $ns\sigma_g$ and $nd\lambda_g$ series.[3]

Since N_2O is almost homonuclear, it might be regarded as belonging to the $D_{\infty h}$ point group and therefore as having inversion symmetry. This assumption was used by Patsilinakou *et al.*[17] to explain the relative intensities of the 0_0^0, 2_0^1, and 2_1^0 bands associated with the $3p\sigma\ ^1\Pi$ state in the 2+1 and 3+1 REMPI spectrum. The 0_0^0 band is strong in the 3+1 REMPI spectrum and weak in the 2+1 REMPI spectrum. In contrast with this, the 2_0^1 and 2_1^0 bands are stronger in the 2+1 REMPI spectrum than in the 3+1 REMPI spectrum. The $3p\sigma\ ^1\Pi$ state is formed out of an $X\ ^2\Pi_{g}$ ion core and a $3p\sigma_{u}$ Rydberg orbital. The direct product is ungerade so that the (0,0,0) $X\ ^1\Sigma_{g}^{+}\rightarrow$(0,0,0) $3p\sigma\ ^1\Pi_{u}$ transition should be allowed in one- and three-photon absorption and forbidden in two-photon absorption. In the same way, 2_0^1 and 2_1^0 transitions can be regarded as effective $g\rightarrow g$ and $u\rightarrow u$ promotions, respectively, that should only be allowed in two-photon absorption.

It is interesting to compare the REMPI spectra of CS_2 with our results for N_2O; validity of the parity selection rules for N_2O would imply that the $ns\sigma$ series is absent from the 3+1 REMPI spectrum, or at least very weak. Our observation of the $ns\sigma$ series as a prominent series in the 3+1 REMPI spectrum, at least comparable in strength with the $np\sigma$ and $np\pi$ series ('g'$\rightarrow$'u'), casts doubt on the validity of parity selection rules based on approximate inversion symmetry.

In the photoelectron spectra recorded at higher excitation energies, a large number of peaks from electrons with low kinetic energy can be observed, as is the case with other molecules.[25,26] A prototypical example is shown in Fig. 5,

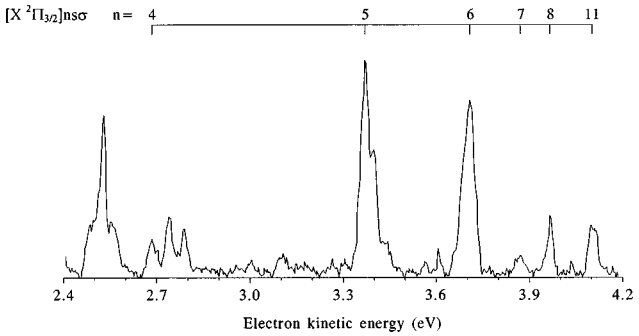

FIG. 5. Photoelectron spectrum resulting from (3+1) REMPI via the $[X\ ^2\Pi_{3/2}]11s\sigma$ state.

which displays the photoelectron spectrum obtained for ionization via the $[X\ ^2\Pi_{3/2}]11s\sigma(v'=0)$ Rydberg state. On the basis of the $\Delta v=v^+-v'=0$ propensity rule for ionization of Rydberg states, one would *a priori* expect that ionization would lead to ions in their vibrationless $X\ ^2\Pi_{3/2}$ ground state. Figure 5 shows, in contrast, that photoionization results predominantly in photoions with a large amount of vibrational energy. The explanation for this apparent contradiction is found in the role of vibronic coupling between the $[X\ ^2\Pi_{3/2}]11s\sigma(\mathbf{v}'=\mathbf{0})$ level and nearly coincident vibronic levels of lower-lying Rydberg states. If such a vibronic coupling is strong enough, a description of the state that is ionized as $|[X\ ^2\Pi_{3/2}]11s\sigma>|\mathbf{v}'=\mathbf{0})$ is not accurate, but should be corrected to $|[X\ ^2\Pi_{3/2}]11s\sigma>|\mathbf{v}'=\mathbf{0})+\Sigma_i\mu_i|[X\ ^2\Pi_{3/2}]\times n_i\ell_i\lambda_i>|v'_{1,i},v'_{2,i},v'_{3,i})$. Assuming $\Delta v=0$ ionization, ionization of the latter wavefunction will not only give rise to ions in their vibrationless ground state, but also to ions with an internal energy given by (v_1^+,v_2^+,v_3^+). Under the usual assumption that vibrational frequencies in the Rydberg state are close to the vibrational frequencies of the ionic core upon which the Rydberg state is built, the difference between the kinetic energies of electrons associated with ions generated in the (v_1^+,v_2^+,v_3^+) and $\mathbf{v}^+=\mathbf{0}$ levels thus directly reflects the difference in the electronic excitation energies of the $[X\ ^2\Pi_{3/2}]11s\sigma$ and the vibronically coupled $[X\ ^2\Pi_{3/2}]n_i\ell_i\lambda_i$ Rydberg states. In this way, a photoelectron spectrum recorded for ionization via higher-lying Rydberg states allows the direct observation of many lower-lying Rydberg states.[25,26] For instance, the photoelectron spectrum displayed in Fig. 5 shows a large part of the $[X\ ^2\Pi_{3/2}]ns\sigma$ series. The principle of this vibronic mixing is schematically shown in Fig. 6. The $[X\ ^2\Pi_{3/2}]ns\sigma$ states which couple with the $[X\ ^2\Pi_{3/2}]11s\sigma(\mathbf{v}'=\mathbf{0})$ state are indicated as quasicontinua. Even for Rydberg states relatively close to $[X\ ^2\Pi_{3/2}]11s\sigma$, e.g., the $[X\ ^2\Pi_{3/2}]8s\sigma$ state, the number of vibronic levels which can couple is quite significant. This is partly due to the fact that for the linear N_2O molecule, Renner–Teller coupling is operative, leading to several vibronic states arising from the coupling between degenerate electronic states and one or more quanta of the bending vibration ν_2.

In the present case, states are observed that belong predominantly to the same series, although weaker vibronic coupling with other series is also observed. Vibronic cou-

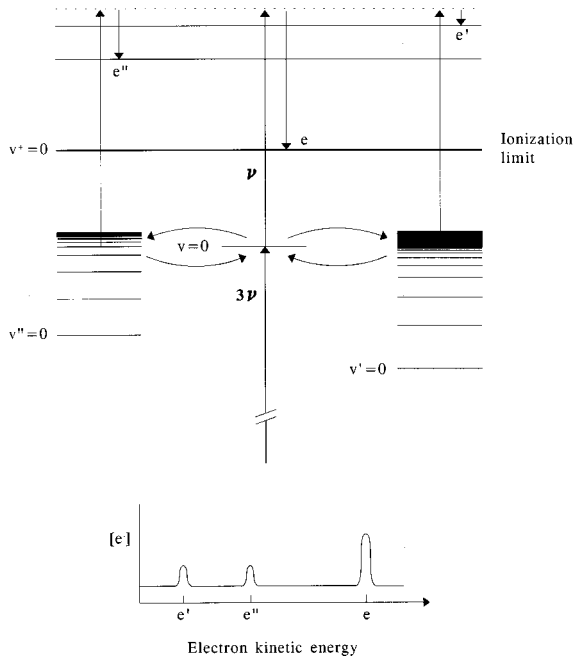

FIG. 6. Schematic illustration showing vibronic mixing between the three-photon resonant origin ($v=0$) level of one Rydberg state and accidentally near-resonant excited vibrational levels of two lower-lying Rydberg states, whose origins are labeled as $v'=0$ and $v''=0$, respectively.

pling thus enables us to confirm the electronic excitation energies of Rydberg states observed in the REMPI excitation spectrum. At the same time, it enables the observation of Rydberg states whose $\Delta v=0$ transitions cannot be observed in the REMPI excitation spectrum due to low dye gain at those excitation energies. For example, in the present study the origin transitions to the $[X\ ^2\Pi_{3/2,1/2}]5p\sigma,6p\sigma$ states could not be observed, but photoelectron spectra obtained for ionization via higher-lying Rydberg states show peaks that can consistently be interpreted as deriving from ionization of vibronic levels of the $[X\ ^2\Pi_{3/2,1/2}]5p\sigma,6p\sigma$ Rydberg states.

IV. CONCLUSIONS

The application of three-photon excitation spectroscopy in combination with mass-resolved ion and kinetic energy-resolved electron detection has led to a detailed characterization of Rydberg states of N_2O in the wavelength region from 80 000 cm^{-1} up to the lowest ionization limit at 103 963 cm^{-1}. We were able to confirm many of the earlier assignments[17,18] of vibronic structure associated with the $3p\sigma'\Pi$ state in the 80 000–90 000 cm^{-1} energy range. However, the photoelectron spectrum of the resonance at 82 725 cm^{-1} shows that this resonance, which was formerly assigned as a 3_1^1 band, is the transition to the vibrationless $3p\sigma\ ^3\Pi$ state. In the spectral region from 90 000 cm^{-1} up to the lowest IE, we have observed 17 origins which were either not assigned earlier or are reassigned now.

Intensities and splittings of the $\Omega_c=1/2$ and $\Omega_c=3/2$ states in the REMP1 spectrum, as well as the presence of only one spin-orbit component in most of the photoelectron spectra, indicate that Hund's case *c* representation is appropriate for all observed Rydberg states, except for the $[X\ ^2\Pi_{1/2,3/2}]3p\sigma$ and the $[X\ ^2\Pi_{1/2,3/2}]4p\pi$ states. The photoelectron spectra recorded at higher-lying resonances show photoelectrons, which can be attributed to vibronic coupling of the resonance with the near-resonant vibronic manifolds built on lower-lying origins. In this way, large parts of Rydberg series are observed in single photoelectron spectra.

ACKNOWLEDGMENT

The authors are grateful to the Netherlands Organization for Scientific Research (NWO) for equipment grants and for financial support (C.R.S).

[1] M. R. Dobber, W. J. Buma, and C. A. de Lange, J. Chem. Phys. **101**, 9303 (1994).
[2] R. A. Morgan, A. J. Orr-Ewing, D. Ascenzi, M. N. R. Ashfold, W. J. Buma, C. R. Scheper, and C. A. de Lange, J. Chem. Phys. **105**, 2141 (1996).
[3] R. A. Morgan, M. A. Baldwin, A. J. Orr-Ewing, M. N. R. Ashfold, W. J. Buma, J. B. Milan, and C. A. de Lange, J. Chem. Phys. **104**, 6117 (1996).
[4] P. J. Crutzen, J. Geophys. Res. **76**, 7311 (1971).
[5] R. K. Lyon, J. C. Kramlich, and J. A. Cole, Environ. Sci. Technol. **23**, 392 (1989).
[6] Y. Tanaka, A. S. Jursa, and F. J. LeBlanc, J. Chem. Phys. **32**, 1205 (1960).
[7] D. W. Turner, C. Baker, A. D. Baker, and C. R. Brundle, *Molecular Photoelectron Spectroscopy* (Wiley, London, 1970).
[8] K. Watanabe, J. Chem. Phys. **26**, 542 (1957).
[9] J. Berkowitz and J. H. D. Eland, J. Chem. Phys. **67**, 2740 (1977).
[10] R. T. Wiedmann, E. R. Grant, R. G. Tonkyn, and M. G. White, J. Chem. Phys. **95**, 746 (1991).
[11] G. Herzberg, *Electronic Spectra of Polyatomic Molecules* (Van Nostrand Reinhold, New York, 1996).
[12] J. F. M. Aarts and J. H. Callomon, Chem. Phys. Lett. **91**, 419 (1982).
[13] A. B. F. Duncan, J. Chem. Phys. **4**, 638 (1936).
[14] M. Zelikoff, K. Watanabe, and E. C. Y. Inn, J. Chem. Phys. **21**, 1643 (1953).
[15] E. N. Lassettre, A. Skerbele, M. A. Dillon, and K. J. Ross, J. Chem. Phys. **48**, 5066 (1968).
[16] R. H. Hueber, R. J. Celotta, S. R. Mielczarek, and C. E. Kuyatt, J. Chem. Phys. **63**, 4490 (1975).
[17] E. Patsilinakou, R. T. Wiedmann, C. Fotakis, and E. R. Grant, J. Chem. Phys. **91**, 3916 (1989).
[18] M. G. Szarka and S. C. Wallace, J. Chem. Phys. **95**, 2336 (1991).
[19] M. Ukai, K. Kameta, S. Machida, N. Kouchi, Y. Hatano, and K. Tanaka, J. Chem. Phys. **101**, 5473 (1994).
[20] E. Lindholm, Ark. Fys. **40**, 97 (1968).
[21] B. G. Koenders, D. M. Wieringa, K. E. Drabe, and C. A. de Lange, Chem. Phys. **118**, 113 (1987).
[22] C. E. Moore, *Atomic Energy Levels*, Natl. Bur. Stand. (U.S.) circ. 467 (U.S. GPO, Washington, D.C.), Vol. II (1952) and Vol. III (1958).
[23] T. C. Betts and V. McKoy, J. Chem. Phys. **60**, 2947 (1974).
[24] H. Lefebvre-Brion and R. W. Field, *Perturbations in the Spectra of Diatomic Molecules* (Academic, Orlando, FL, 1986).
[25] R. A. Morgan, P. Puyuelo, J. D. Howe, M. N. R. Ashfold, W. J. Buma, N. P. L. Wales, and C. A. de Lange, J. Chem. Soc., Faraday Trans. **91**, 2715 (1995).
[26] R. A. Morgan, A. J. Orr-Ewing, M. N. R. Ashfold, W. J. Buma, N. P. L. Wales, and C. A. de Lange, J. Chem. Soc., Faraday Trans. **91**, 3339 (1995).
[27] J. H. Callomon and F. Creutzberg, Philos. Trans. R. Soc. London, Ser. A **277**, 157 (1974).